Supporting Information

Low-Temperature All-Solution-Processed Transparent Silver Nanowire-Polymer/AZO Nanoparticles Composite Electrodes for Efficient ITO-Free Polymer Solar Cells

Xiaoqin Zhang,[†,‡] Jiang Wu,[†] Jiantai Wang,[†,‡] Qingqing Yang,[†,‡] Baohua Zhang,[†] and Zhiyuan Xie*[†]

[†] State Key Laboratory of Polymer Physics and Chemistry, Changchun Institute of Applied Chemistry, Chinese Academy of Sciences, Changchun 130022, P. R. China

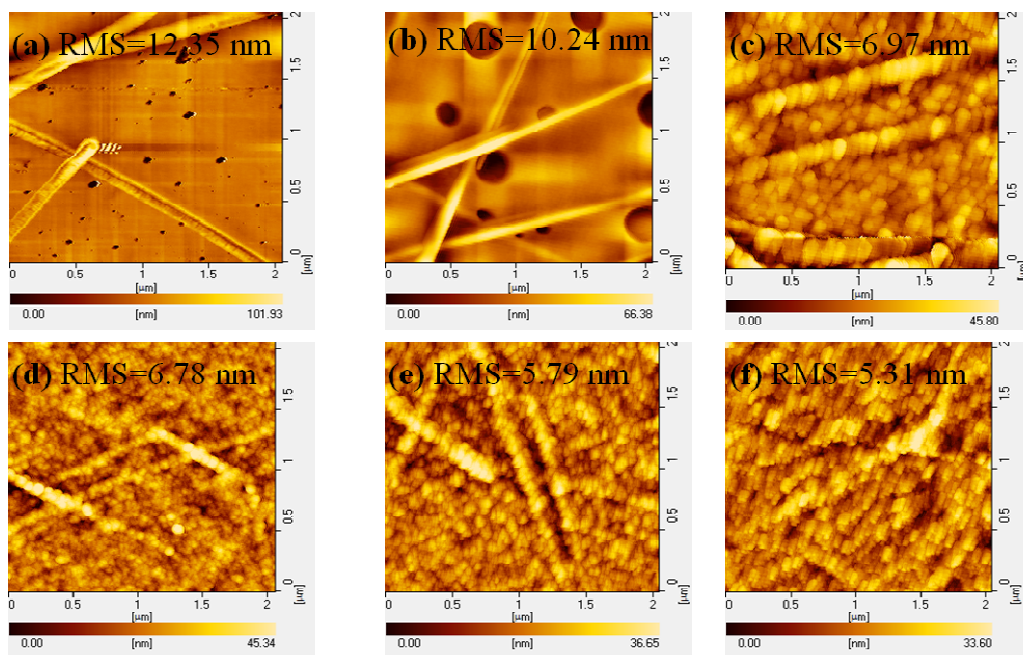[‡] University of Chinese Academy of Sciences, Beijing 100039, P. R. China

Figure S1. AFM topographic images of the various AgNW-based transparent conductive films: (a) pristine AgNW, (b) AgNW blended with PVB, and (c-f) APA composite films covered with 1-layer, 2-layer, 3-layer and 4-layer AZO prepared with doctor-blade coating.

Figure S2. Cross-section SEM images of various AgNW-based films: (a) pristine AgNW, (b) AgNW blended with PVB, and (c-f) APA composite films covered with 1-layer, 2-layer, 3-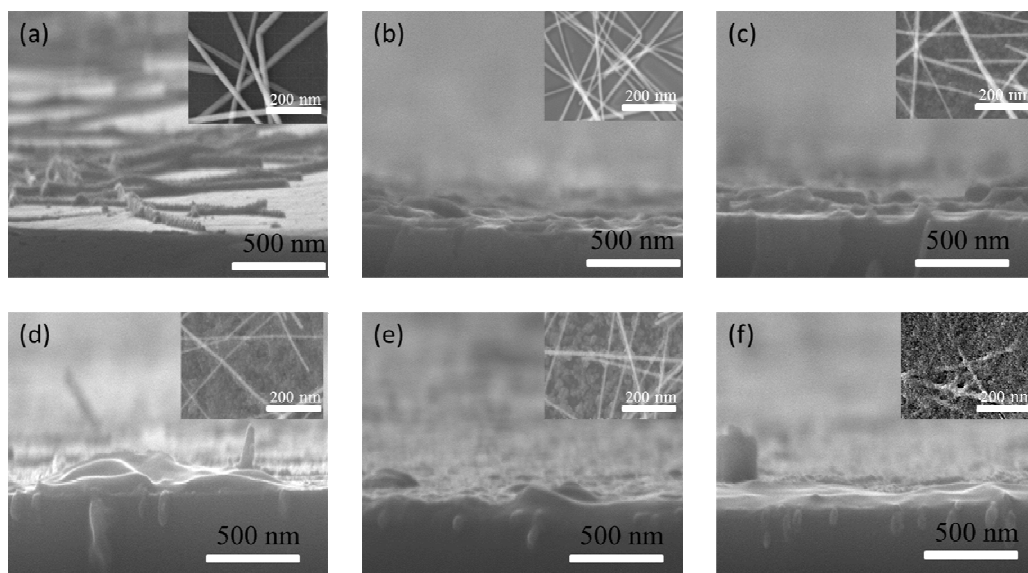layer and 4-layer AZO prepared with doctor-blade coating. The insets in (a-f) are the corresponding SEM images in plain view.
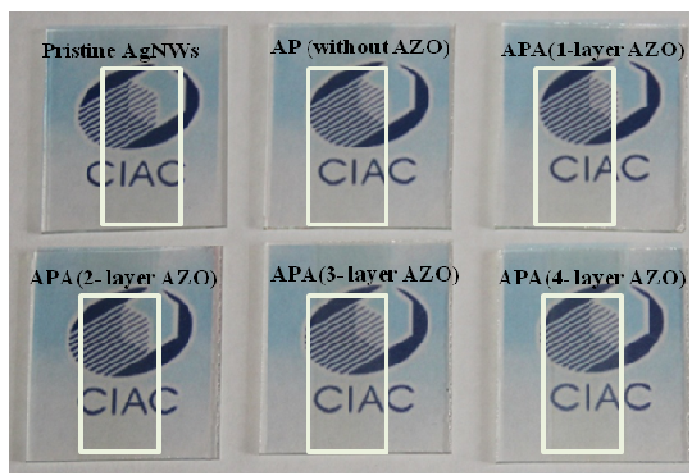
Figure S3. Photographs of the patterned AgNW-based transparent electrodes on glass substrates prepared with doctor-blade coating (the transparent electrodes are marked with blocks).
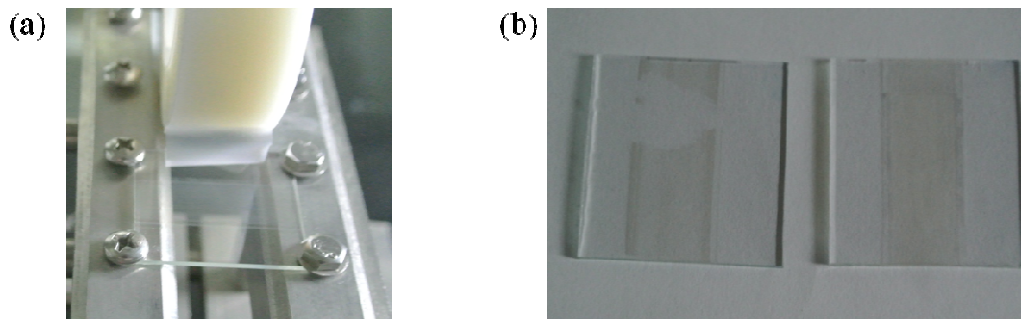
Figure S4. (a) The photograph of tape test using 3M Scotch tape. (b) Photographs of pristine AgNW destroyed by finger friction (left) and APA composite electrode after 500 cycles of tape test (right).
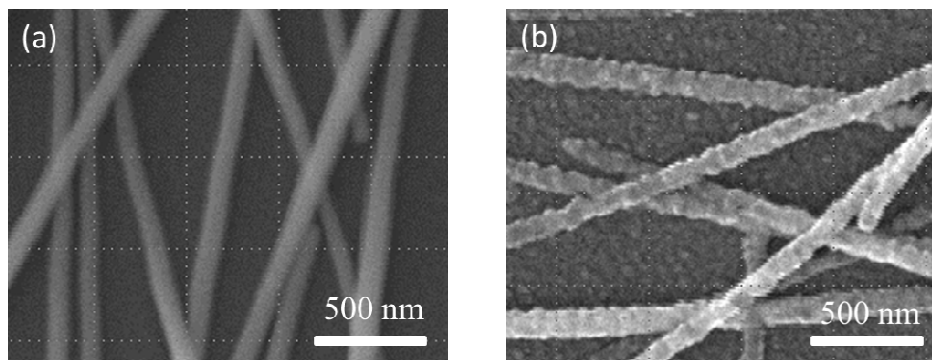
Figure S5. The SEM images of the AgNWs (a) before and (b) after exposure for two months under ambient conditions.
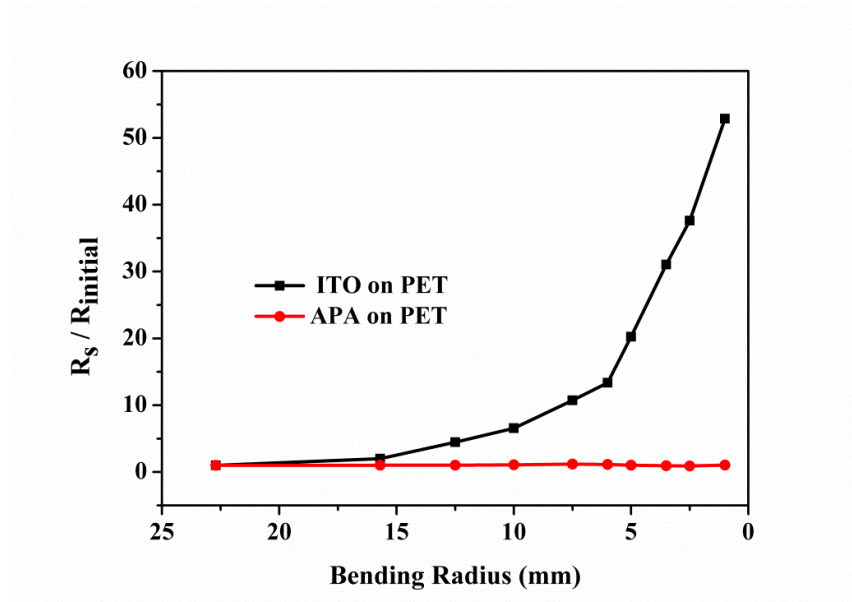
Figure S6. Rs changes relative to its initial value for the APA composite/PET substrate and

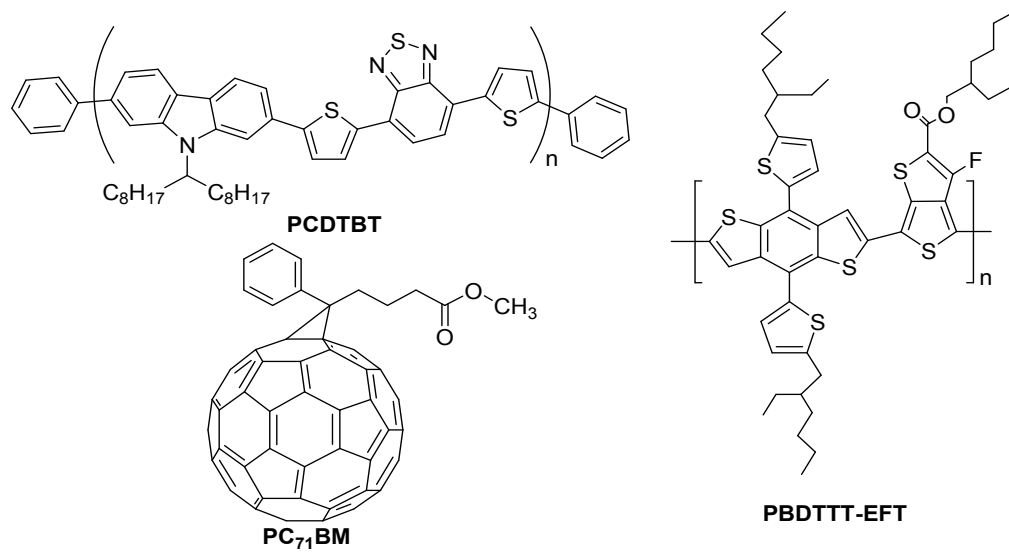the commercial ITO/PET substrate as a function of the bending radius.

Figure S7. Chemical structures of PCDTBT, PBDTTT-EFT and PC$_{71}$BM used in this study.
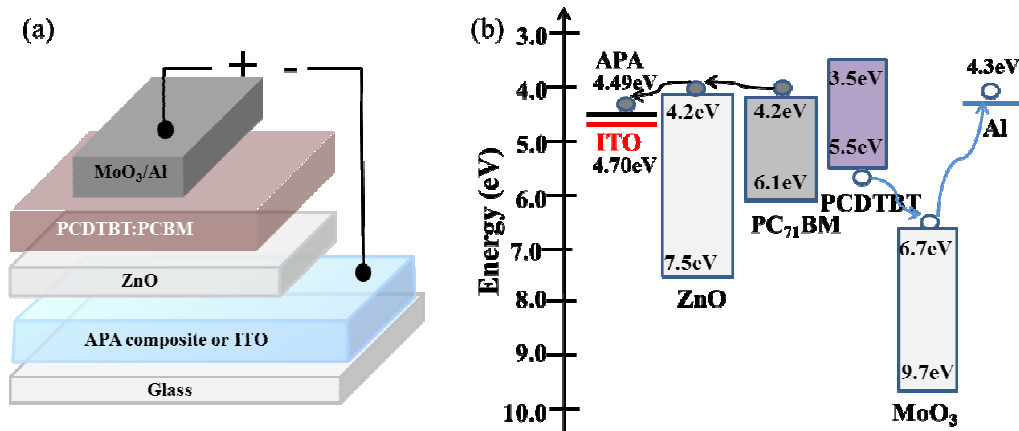
Figure S8. (a) Device architecture of the inverted PCDTBT:$PC_{71}BM$ PSCs employing the APA composite or ITO as the cathode. (b) Energy level diagram of the PCDTBT:$PC_{71}BM$ PSCs.

The thermally evaporated MoO_3 is used as the hole-injection layer in the inverted PSCs. The edge of the occupied valence band of MoO_3 is 2.82 eV below Fermi level, corresponding to ionization energy = 9.68 eV. [S1-S2] IPES measurements on the same sample place the edge of the unoccupied state band at 0.16 eV above Fermi level, and yield an electron affinity of 6.7 eV and an band gap of 3 eV. MoO_3 is not a *p*-type oxide but rather an n-type material with very high work-function, high electron affinity and very high ionization energy. Holes are extracted via LUMO of MoO_3.

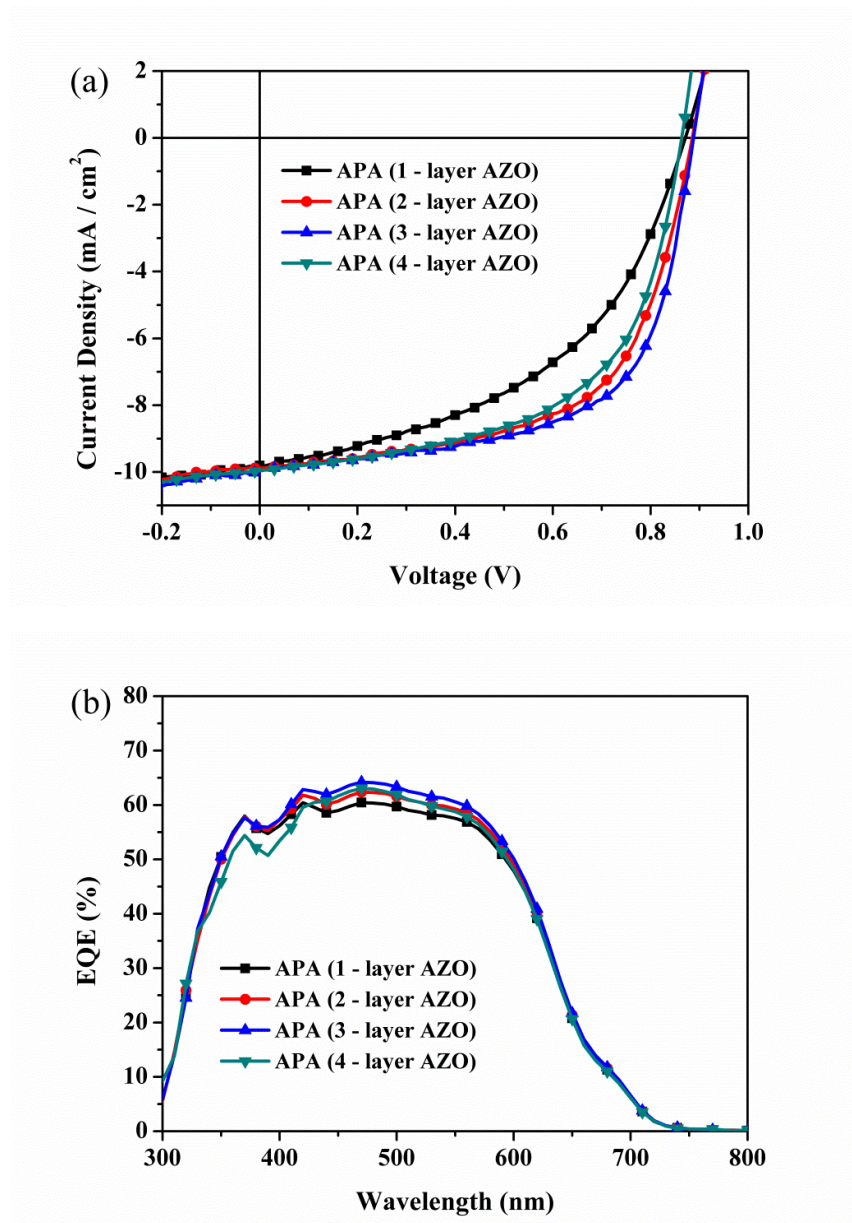**Figure S9.** (a) J-V characteristics of inverted PSCs devices based on APA composite electrodes with different layers AZO nanoparticles. (b) EQE of the PSCs based APA composite electrodes.
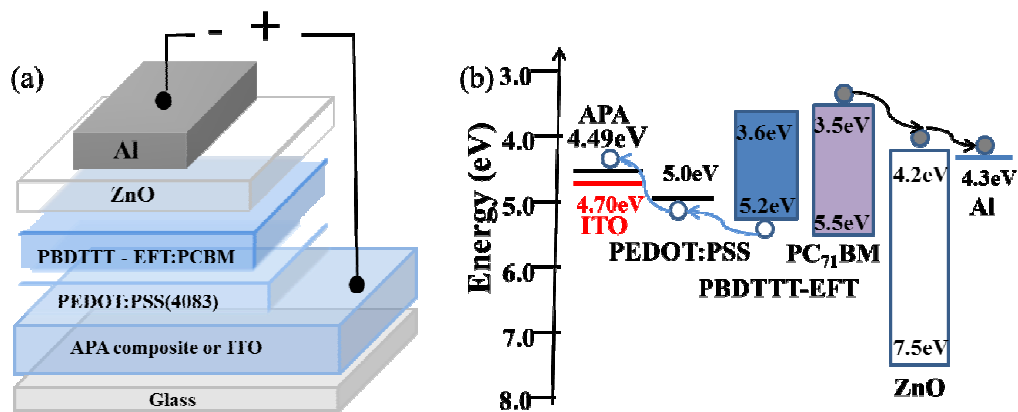
Figure S10. (a) Device architecture of the conventional PBDTTT-EFT:PC_{71}BM PSCs employing the APA composite or ITO as the anode. (b) Energy level diagram of the conventional PSCs based on PBDTTT-EFT:PC_{71}BM blend.

Table S1. Photovoltaic parameters of the PCDTBT: PC$_{71}$BM PSCs employing the APA composites with different layers of AZO nanoparticles or ITO as transparent electrodes.

Electrode	V_{OC} (V)	J_{SC} (mA/cm^2)	FF (%)	PCE^a (%)	R_S (Ω cm^2)	R_{SH} (Ω cm^2)	Cal $J_{SC}{}^b$ (mA/cm^2)
APA(1-layer AZO)	0.87±0.02	9.84±0.15	47.75±1.12	4.11±0.19	20.77	411.26	9.45
APA(2-layer AZO)	0.88±0.01	9.89±0.32	58.40±0.74	5.10±0.24	12.61	712.55	9.54
APA(3-layer AZO)	0.88±0.01	9.98±0.33	61.29±0.59	5.40±0.14	10.03	513.11	9.75
APA(4-layer AZO)	0.86±0.01	9.90±0.21	55.84±2.23	4.77±0.25	10.90	627.84	9.65

^{a}The values are the average of 10 devices; ^{b}The J_{SC} values are calculated from EQE spectra.

Table S2. Photovoltaic parameters of the conventional PBDTTT-EFT:PC$_{71}$BM PSCs fabricated using the APA composite or ITO as the transparent electrode.

Electrode	V_{OC} (V)	J_{SC} (mA/cm^2)	FF (%)	PCE[a] (%)	R_S (Ω cm^2)	R_{SH} (Ω cm^2)	Cal J_{SC}[b] (mA/cm^2)
APA	0.77±0.01	18.76±0.26	61.00±0.48	8.84±0.32	7.29	733.68	18.12
ITO	0.78±0.01	19.41±0.13	62.74±0.12	9.52±0.05	6.17	751.46	19.14

[a]The values are the average of 10 devices; [b]The Cal J_{SC} values are calculated from EQE spectra.

References

[S1] Kröger. M; Hamwi. S; Meyer. J; Riedl. T; Kowalsky. W; Kahn. A. Role of the Deep-Lying Electronic States of MoO_3 in the Enhancement of Hole-Injection in Organic Thin Films. *Appl. Phys. Lett.* **2009**, *95*, 123301.

[S2] Meyer. J; Hamwi. S; Kröger. M; Kowalsky. W; Riedl. T; Kahn. Transition Metal Oxides for Organic Electronics: Energetics, Device Physics and Applications. *Adv. Mater.* **2012**, *24*, 5408–5427.